Contents lists available at ScienceDirect

Saudi Pharmaceutical Journal

journal homepage: www.sciencedirect.com

Original article

The potential antiepileptic activity of astaxanthin in epileptic rats treated with valproic acid

Yussra Ata Yaseen Abdulqader [a,b], Hala Salah Abdel Kawy [a], Huda Mohammed Alkreathy [a,*], Nisreen Abdullah Rajeh [c]

[a] Department of Pharmacology, Faculty of Medicine, King Abdulaziz University, Jeddah, Saudi Arabia
[b] King Abdullah Medical Complex, Jeddah, Saudi Arabia
[c] Department of Anatomy, Faculty of Medicine, King Abdulaziz University, Jeddah, Saudi Arabia

ARTICLE INFO

ABSTRACT

Objectives: Epilepsy is a neurological disease characterized by sudden, abnormal, and hyper- discharges in the central nervous system (CNS). Valproic acid (VPA) is commonly used as a broad-spectrum antiepileptic therapeutic. However, in many cases, patients develop resistance to VPA treatment due to overwhelming oxidative stress, which in turn might be a major catalyst for disease progression. Therefore, antioxidants can potentially become therapeutic agents by counteracting reactive oxygen species (ROS)-mediated damage. The present study is aimed to evaluate the potential antiepileptic effect of astaxanthin (ASTA) in pentylenetetrazol (PTZ) induced epileptic model rats that are chronically treated with VPA for 8 weeks.

Method: Fifty-male Wistar rats were randomly divided into five groups: Non-PTZ group, PTZ, PTZ/VPA, PTZ/ASTA, and PTZ/VPA/ASTA treated groups.

Results: PTZ/VPA treated group showed a neuroprotective effect with improvement in antioxidant levels, behavioral test, and histopathological changes induced by PTZ. VPA also exhibited an anti-inflammatory effect as its treatment resulted in the reduction of tumor necrosis factor-α (TNF-α). ASTA exhibited an anticonvulsant effect and enhanced anti-inflammatory effect as compared to VPA. During the combined therapy, ASTA potentiated the antiepileptic effect of the VPA by reducing the oxidative stress and TNF-α as well as increased the glutathione (GSH) levels. Also, there were substantial improvements in the behavioral and histopathological changes in the VPA/ASTA treated group as compared to the VPA treated group.

Conclusion: ASTA could have an antiepileptic and anti-inflammatory effect by reducing ROS generation. Therefore, co-administration of both the therapeutics (VPA/ASTA) has a synergistic effect in treating epilepsy and could potentially minimize recurrence and/or exacerbation of seizures.

Production and hosting by Elsevier

1. Introduction

Epilepsy is a prevalent chronic neurological disease that has affected around 50 million people worldwide and accounts for 1% of the global disease burden (World Health Organization, 2019). Notably, epilepsy has ranked top among the neurological diseases in primary health care throughout the Eastern Mediterranean countries. Similarly, in Saudi Arabia, the prevalence of epilepsy is considerably high, with estimated 23,700 patients diagnosed with the disease. On average, 6.5 epileptic patients are identified among 1000 people (Al-Qahtani et al., 2018).

Reactive oxygen species and oxidative stress are associated with the development of epileptic seizures. The imbalance

Y. Ata Yaseen Abdulqader, Hala Salah Abdel Kawy, H. Mohammed Alkreathy et al.

Saudi Pharmaceutical Journal 29 (2021) 418–426

between reactive oxygen species (ROS) generation and the system's inability to eliminate reactive intermediates is termed oxidative stress (Nita and Grzybowski, 2016). Due to high oxygen consumption and a weak antioxidant system, brain tissue is easily exposed to oxidative damage than other tissue types, resulting in cell death (Shin et al., 2011). Moreover, seizure activity causes increased free radicals and downregulates antioxidant defense mechanisms (Mendez-Armenta et al., 2014). Therefore, epileptic seizure mediated oxidative stress is a significant catalyst for recurrent seizures and can also exacerbate the consequences. Oxidative damage and consequent neuronal cell death have common pathogenic processes that contribute significantly to epileptogenesis. They also participate in the initiation and propagation of spontaneous and recurrent seizures. Thus, increased mitochondrial oxidative stress and mitochondrial dysfunction may be the final common pathway underlying these neuropathological conditions. It is also possible that they contribute to epileptogenesis, meaning that they are capable of causing chronic acquired epilepsy (Rowley et al., 2015).

An increase in the hippocampal glutamate levels resulted in considerable neuronal death and microglial activation in the hippocampal CA3 regions and increased pro-inflammatory cytokine production (Chang et al., 2018). In addition, TNF-α is mainly produced by activated microglia and astrocytes in response to various stimuli, including infection and injury (Liu et al. 2014).

Valproic acid is a commonly used broad-spectrum antiepileptic drug (AED) but, its application leads to numerous side effects such as teratogenicity (Jentink et al., 2010). Moreover, Grewal et al. summarized that oxidative stress reduces the patients' response to AEDs by modulating the ABC transporters responsible for the drug uptake inside the cell (Grewal et al., 2017). Therefore, the significant role of ROS in the development of epileptic seizures has stimulated investigations into the potential neuroprotective effects of antioxidants.

Astaxanthin (ASTA) is an effective antioxidant that has recently come into focus. Many studies have shown astaxanthin to be a powerful antioxidant, which directly or indirectly reduces the effect of oxidation and oxidizing damage without any harmful side effects (Ambati et al., 2014).

The role of oxidative stress in epileptogenesis is emerging and has recently become the subject of extensive research. Accordingly, the present study was performed using the rat model of PTZ-induced epilepsy and the role of antioxidant and mitochondrial cytoprotective agent ASTA was investigated to understand the impact of antioxidants on the process of epileptogenesis and consequently on the antiepileptic activity of VPA. The study also aimed to investigate the changes in ROS markers in neuronal and hepatic tissues, motor coordination, glutamate concentration in the brain, and pro-inflammatory marker, urea, uric acid, and liver enzymes in the serum. The impact of ASTA on that changes and subsequent adverse histopathological changes (hippocampal changes, and hepatoxicity) was determined in an attempt to describe a possible protective effect of antioxidants against the hippocampal changes and hepatotoxic effects (if any) that VPA might induce.

2. Material and methods

Valproic acid was obtained from Sigma Aldrich (CAS number: 1069-66-5), while Astaxanthin (Astaxanthin-Enriched *Haematococcus pluvialis* powder 5% (AstaZine)) was a gift from Algea health sciences INC; A BGG company (CAS number 472-61-7). Both were dissolved in 50 mg/ml distilled water for oral administration.

2.1. Study design

Fifty male Wistar rats, 6–8 weeks old with 180–250 g body weight, were chosen for the study. Animals were housed in a standard clear polycarbonate cage with free access to food and water. Animals were kept on a 12-h light–dark cycle daily, in a controlled environment at a temperature of 25 °C, complying with ethical standards. All experiments were conducted during the light phase, from 10:00 A.M. to 4:00 P.M. The experimental protocol was approved by the institutional of Animals Care and Use Committee (ACUC) and Research Ethics Committee (REC), reference number-595-17, Faculty of medicine, King Abdulaziz University, Jeddah, Saudi Arabia.

Rats were randomly divided into five groups: **Group A**:(control-negative) received vehicle for VPA and ASTA by oral gavage daily and vehicle for PTZ by intraperitoneally three times a week, **Group B**: (control-positive) received vehicle for VPA and ASTA by oral gavage daily and 30 mg/kg of PTZ (Atack et al., 2000) by intraperitoneally three times a week, **Group C**: received 500 mg/kg of valproic acid (El-Mowafy et al., 2016) by oral gavage daily and PTZ by intraperitoneally three times a week, **Group D**: received 100 mg/kg of astaxanthin (Chang et al., 2018) by oral gavage daily and, PTZ by intraperitoneally three times a week, and **Group E**: received valproic acid, astaxanthin by oral gavage daily 2 h apart and PTZ by intraperitoneally three times a week.

Orally administered drugs were suspended in 0.1% methylcellulose. At the start of the experiment, animals received oral prophylactic drugs, and on the next day, they received PTZ injection one hour after administering oral drugs. The duration of the experiment was up to 8 weeks when the rats showed full kindling. All animals were weighed weekly and the drug doses were adjusted accordingly.

2.2. Assessment of epileptogenesis induced by PTZ kindling

For PTZ kindling, a sub-convulsant dose of PTZ 30 mg/kg body weight was injected intraperitoneally three times a week. The animals were observed for convulsive behavior for 30 min after each PTZ administration. Seizure activity was evaluated using the following scale (Racine, 1972): Stage 0: no response, stage 1: hyperactivity, vibrissae twitching, stage 2: head nodding, head clonus and myoclonic jerk, stage 3: unilateral forelimb clonus, stage 4: rearing with bilateral forelimb clonus, stage 5: generalized tonic-clonic seizure (GTCS) with loss of postural control. Animals that reached stage 4 or 5 of seizure on three consecutive trials were considered full kindling (Hussein et al., 2018). Latency to the onset of (GTCS) and duration of (GTCS) were recorded immediately after the last dose of PTZ was administered at the end of 8th week. Also, the mortality rate among the animals was monitored.

2.3. Rotarod performance test

All rats were evaluated for motor coordination (locomotor) using a Rotarod machine. It measured balance, coordination, and motor control of the animals. The procedure was done after administering the last PTZ injection. Animals were placed on the rotating rod (7 cm diameter) in separate lanes, at a constant speed of 12 rpm. Time spent on the rod was measured for 90 s (Latency to fall) (Huang et al., 2002).

2.4. Biochemical measurements

Post behavioral assessment, animals were anesthetized by administering 1.2 gm/kg of urethane intraperitoneal injection (Sedky et al., 2017). Subsequently, blood samples were collected from the ophthalmic venous plexus through retro-orbital

Y. Ata Yaseen Abdulqader, Hala Salah Abdel Kawy, H. Mohammed Alkreathy et al.

Saudi Pharmaceutical Journal 29 (2021) 418–426

approach, and the animals were decapitated. The brain tissue was isolated and divided into two parts; one was stored at −80 °C for biochemical assessment, and the second was kept in 10% formaldehyde for histological studies.

2.4.1. Biochemical measurements in serum

2.4.1.1. Urea content. It was performed using Urea assay kit (Urease method) (MyBioSource, San Diego, CA, USA). Urease hydrolyzes urea into ammonium ion and carbon dioxide. Ammonium ions react with phenol chromogenic agent to yield a blue color substance, measured by a colorimetric assay at 640 nm.

2.4.1.2. Tumor necrosis factor-α (TNF-α). The assay was performed using tumor necrosis factor-a PicoKine (TNF-α) ELISA kit (MyBioSource, San Diego, CA, USA) for the quantitative detection of rat TNF-α in serum, employing sandwich ELISA technique. The experiment was performed following the manufacturer's instructions.

2.4.2. Biochemical measurements in the hippocampal tissue homogenates

2.4.2.1. Detection of total protein. The total protein content in the supernatant of hippocampal homogenate samples was measured using a Bradford protein assay kit (MyBioSource, San Diego, CA, USA), following manufacturer's instructions.

2.4.2.2. Antioxidant and oxidative stress markers.
1. Reduced glutathione (GSH) estimation was done using rat reduced glutathione (RGLU) ELISA kit (MyBioSource, San Diego, CA, USA). Experiments were performed following the manufacturer's instructions.
2. Lipid peroxidation (MDA) assay was done using Rat Malondialdehyde (MDA) ELISA kit (MyBioSource, San Diego, CA, USA). This assay allows the quantitative determination of rat MDA in tissue homogenate employing competitive enzyme immunoassay technique. Manufacturer's instructions were followed to perform the experiment.
3. Protein carbonyl (PC) estimation was performed using rat protein carbonyl (PC) ELISA kit (MyBioSource, San Diego, CA, USA). The kit adopts sandwich ELISA technique for estimating protein carbonyl content in the sample. Manufacturers' instructions were followed to perform the experiment.

2.4.2.3. Reactive oxygen species (ROS) estimation. Reactive oxygen species assay kit (MyBioSource, San Diego, CA, USA) was used to measure intracellular ROS in the tissue homogenate. DCFH-DA (2,7- dichlorofluorescein diacetate) reagent gets oxidized in the presence of ROS and emits strong green fluorescence. Excitation and emission wavelengths were kept at 500 nm and 525 nm, respectively.

2.5. Glutamate concentration (Glut) estimation in the hippocampus and cerebral cortex by high performance liquid chromatography (HPLC)

HPLC was used to measure glutamate in cerebral tissue as an indicator of neuro-excitatory activity, using Shimadzu Prominence UFLC (Shimadzu, Tokyo, Japan).
Chromatographic conditions: The settings for the HPLC are provided in Table 1 Fig .1.

2.5.1. Preparation of glutamate standard solutions

Different standard solutions of glutamate were prepared. 1 mg of glutamate powder (L-glutamic −2,3,3,4,4-d5 acid 99.2%-d5, CDN isotopes, EQ Laboratories GmbH, Germany) was dissolved in 1 ml of Millipore water to prepare a stock solution. Further, different concentrations of glutamate solutions were prepared (10 mcg/m1, 1mcg/ml, 0.5 mcg/ml, 0.2mcg/ml, and 0.1 mcg/ml). Final samples were prepared by adding 250 mcl of OPA (o-Phthalaldehyde) solution (22 mg of OPA powder dissolved in 0.5 ml of 100% ethanol) in previously prepared glutamate solutions. After shaking, 0.5 ml of 1 M of sodium sulphate was added, followed by the addition of 9 ml of 0.4 M of sodium borate or boric acid in each vial to a final volume of 750 mcl. The samples were vortexed to allow proper mixing. Subsequently, samples were filtered using a 0.2-μm filter needle and were then injected inside the HPLC vial.

2.5.2. Quantification of glutamate content in the brain tissue by HPLC

Brain tissue samples were homogenized in distilled water and heated at 98 °C for 5 min. The samples were then centrifuged at 10, 000 rpm for 5 min at 4 °C. After centrifugation, pellets were suspended in 1 N NaOH, and the total protein amount was determined using the Lowry method (Lowry et al., 1951). In addition, supernatant was filtered through a 0.22 μm filter, derivatized with OPA solution, and was injected into a C18 column (100X2.1MM, Petra Scientific Technologies L.L.C) (Althobaiti et al., 2016). The glutamate concentration in each sample was estimated by analyzing the peak area compared to the external standard, and the values were normalized to the total protein content.

2.6. Histopathological studies

2.6.1 Hematoxylin and eosin staining were used in the histopathology studies to visualize the nucleus and cytoplasmic inclusions in the clinical specimens.
2.6.2 Nissle's staining was performed using cresyl violet acetate solution, which in turn binds to the ribosomal RNA. Nissle's staining gives the cytoplasm a dark blue and mottled appearance.
2.6.3 Hippocampal Glial fibrillary acidic protein (GFAP) immunohistochemical staining. It serves as a cell-specific marker that distinguishes differentiated astrocytes from other glial cells during the central nervous system development.

2.7. Statistical analysis

Results are expressed as mean ± SEM. Statistical analysis was performed using one-way analysis of variance (ANOVA) with Tukey's post hoc test. $P < 0.05$ was considered significant.

3. Results

3.1. Effect of the test drugs on the course of PTZ kindling in rats

3.1.1. Effect of the test drugs on Racine score in rats subjected to PTZ kindling

PTZ injection resulted in a gradual increase in the Racine Score from 1.73 ± 0.19 in the first week to 4.9 ± 0.03 by the end of the 8th week (Fig. 2). VPA treatment resulted in a significantly ($P < 0.05$) lower Racine Score by the end of the 3rd to the 8th week as compared to PTZ treated rats (Fig. 2). ASTA treatment also resulted in a significantly ($P < 0.05$) lower Racine Score compared to rats receiving PTZ alone from the 3rd week onwards to the 7th week (Fig. 2). In the group receiving the combination of both drugs (VPA/ASTA), a significant ($P < 0.05$) decrease in the Racine Score was observed as compared to PTZ-group from the 3rd week onwards. This group also showed a significant ($p < 0.05$) reduction in Racine Score in the 4th (2.08 ± 0.03 vs. 2.38 ± 0.02) and the 5th week (2.12 ± 0.0 17 vs. 2.7 ± 0.13) as compared to PTZ/VPA treated rats (Fig. 2).

Y. Ata Yaseen Abdulqader, Hala Salah Abdel Kawy, H. Mohammed Alkreathy et al.

Saudi Pharmaceutical Journal 29 (2021) 418–426

Table 1
The Shimadzu prominence UHPLC was set using the following parameters.

|	
Column	C18 HPLC column (100X2.1MM),(Petra Scientific Technologies L.L.C item number# ACE-111-1002)
Mobile Phase	0.1 mM EDTA, 0.1 M Na_2HPO_4,(pH 3.0), 7.5% Methanol
Data acquisition (LC Time program)	10 min
Pump (Flow rate)	0.1 ml/min
Detector	SPD-M30A (Photodiode Array Detector)
Injection volume	10 µl
PDA (Lamp)	D2&W
Rinsing Solution	Methanol: Water (50:50)
Retention Time	Glutamate 3.0 to 6.0 min
The mobile phase and the flow rate were modified to optimize the chromatographic response.	
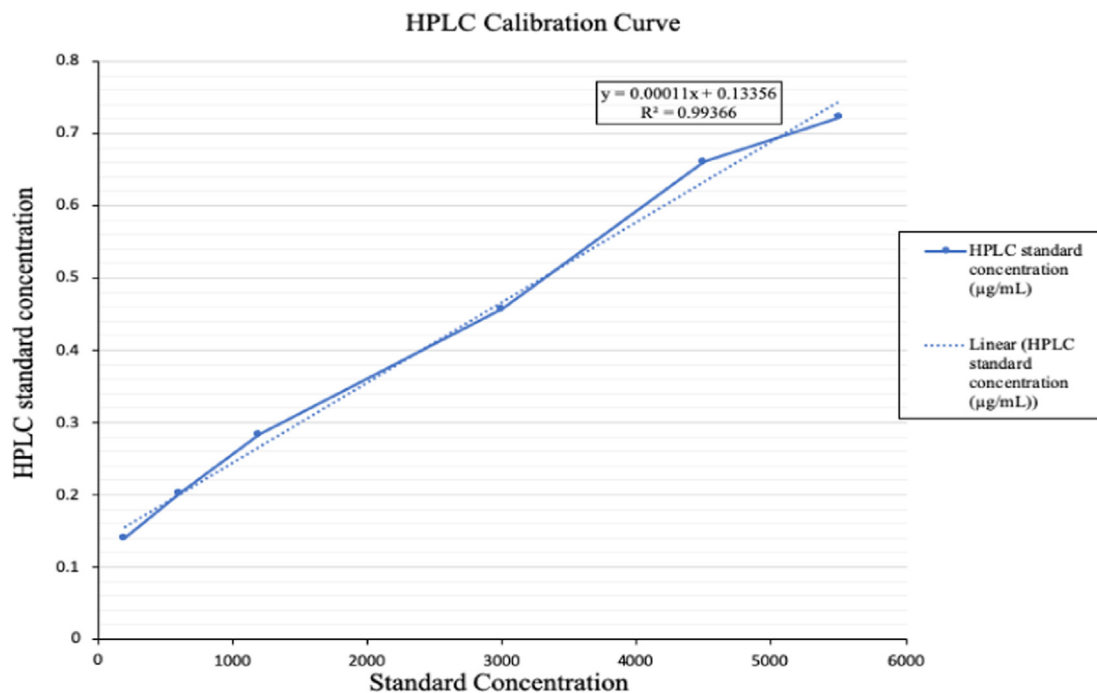
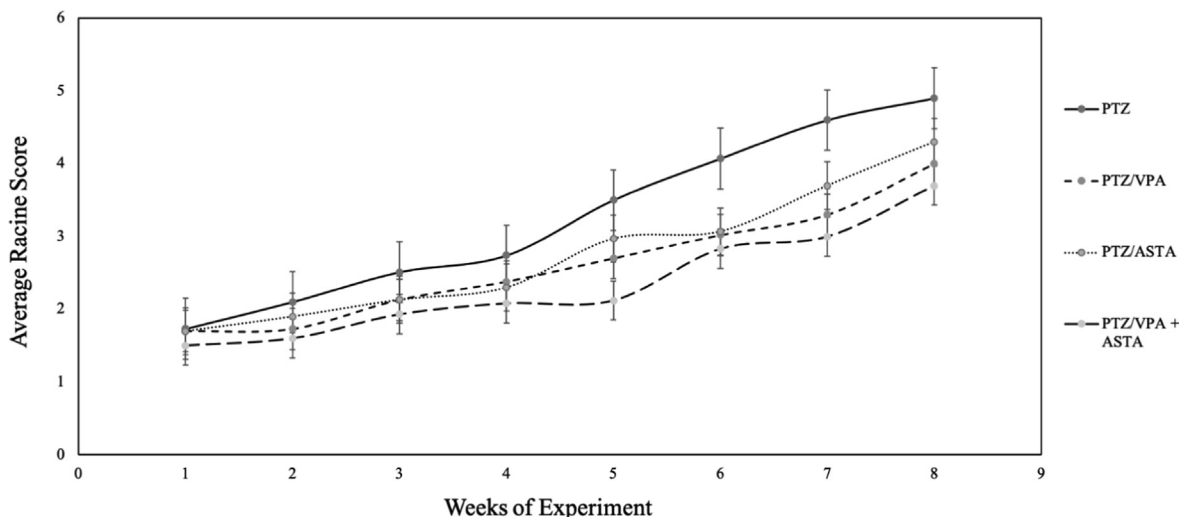**Fig. 1.** HPLC calibration curve.

3.1.2. Effect of the test drugs on PTZ kindling (GTCS; Racine score of 5), latency to the onset of GTCS, duration of GTCS, and mortality rate in rats

PTZ/VPA and PTZ/ASTA treated rats showed a significant ($p < 0.05$) delay in developing PTZ kindling, an increase in the latency to onset of GTCS, and a reduction in the duration of GTCS (Table 2). Furthermore, PTZ/VPA/ASTA group showed a significant ($p < 0.05$) delay in developing PTZ kindling, increased latency to the onset of GTCS, and a more significant reduction in the duration of GTCS as compared to the PTZ/VPA treated group.

Rats subjected to PTZ kindling exhibited a 30% mortality rate, while those treated with VPA or ASTA showed a 20% mortality rate. However, ASTA/VPA treated group reported no animal death.

3.2. Effect of the test drugs on the PTZ induced behavioral modification

In this experiment, PTZ, PTZ/VPA, PTZ/ASTA, and PTZ/VPA/ASTA treated rats showed a significant ($p < 0.05$) reduction in motor and balance coordination as compared to the non-PTZ treated rats, as judged by the time spent on rod (Fig. 3). However, VPA or ASTA

Y. Ata Yaseen Abdulqader, Hala Salah Abdel Kawy, H. Mohammed Alkreathy et al.

Saudi Pharmaceutical Journal 29 (2021) 418–426

Fig. 2. Effect of the test drugs on Racine score in rats treated with PTZ. Data were expressed as mean ± SEM. One-way ANOVA was performed followed by Tukey's multiple comparison test; PTZ: Pentylenetetrazol, VPA: Valproic acid, ASTA: Astaxanthin.*P < 0.05 compared to PTZ, *#P < 0.05 VPA/PTZ + ASTA compared to PTZ/VPA.

Table 2
Effect of the test drugs on the development of PTZ kindling, latency to onset of GTCS, duration of GTCS, and mortality rate in rats at end of the experiment duration (8 weeks).

Animal groups N = 10	Development of PTZ kindling GTCS (in days)	Latency to onset of GTCS (in seconds)	Duration of GTCS (in seconds)	Mortality rate (%)
PTZ	42 ± 1.15	275.33 ± 3.71	19.33 ± 0.88	30%
PTZ /VPA	50 ± 0.58*	377.33 ± 9.84*	10 ± 0.58*	20%
PTZ/ASTA	47 ± 0.58*	373.33 ± 8.41*	13 ± 0.58*	20%
PTZ/ VPA/ASTA	59 ± 1.15*#	459.67 ± 6.64*#	8 ± 0.58*	0

Data were expressed as mean ± SEM, N = number of rats. One-way ANOVA followed by Tukey multiple comparison tests. PTZ: Pentylenetetrazol, VPA: Valproic acid, ASTA: Astaxanthin. GTCS: Generalized tonic-clonic seizures *P < 0.05 compared to PTZ; *#P < 0.05 VPA/PTZ + ASTA compared to PTZ/VPA.
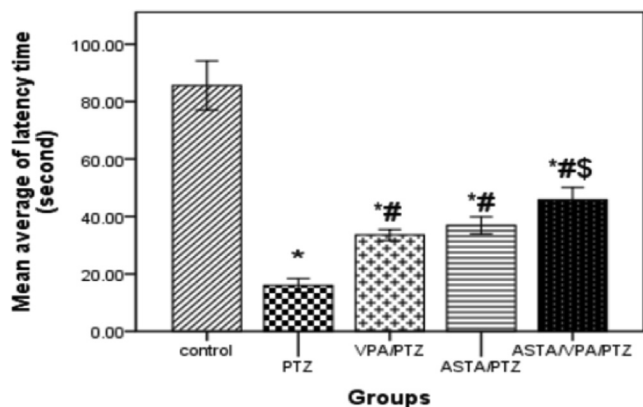
Fig. 3. Effect of the test drugs on Rotarod performance test. Data were expressed as mean ± SEM. One-way ANOVA was performed followed by Tukey's multiple comparison tests. PTZ: Pentylenetetrazol, VPA: Valproic acid, ASTA: Astaxanthin. *P < 0.05 compared to control; *#P < 0.05 compared to PTZ; *#$P < 0.05 PTZ/VPA + ASTA compared to PTZ/VPA.

Table 3
Effect of the test drugs on uric acid, urea, TNF-α concentration measured at the end of experiment (8 weeks).

Animal groups	Serum	
n = 5	TNF-α pg/ml	Urea mg/dl
Control	13.64 ± 1.21	14.5 ± 0.89
PTZ	22.84 ± 0.98 *	41.8 ± 3.54 *
VPA/PTZ	15.8 ± 0.53 #	26.8 ± 3.46 *#
ASTA/PTZ	10.32 ± 0.42 #§	17.4 ± 1.17 #
VPA/PTZ/ASTA	8.9 ± 0.57 *#§	17.8 ± 2.01 #

Data were expressed as mean ± SEM, N = number of animals. One-way ANOVA followed by Tukey multiple comparison tests. PTZ: Pentylenetetrazol, VPA: Valproic acid, ASTA: Astaxanthin. TNF-α: Tumor necrosis factor-α. *P < 0.05 compared to control; # P < 0.05 compared to PTZ; §P < 0.05 PTZ/VPA + ASTA compared to PTZ/VPA.

treated group showed a significant (p < 0.05) increase in motor coordination than the PTZ group. Moreover, PTZ/VPA/ASTA showed a significant (p < 0.05) increase in the coordination compared to PTZ/VPA group (Fig. 3).

3.3. Effects of the test drugs on

3.3.1. Serum urea concentration
PTZ and PTZ/VPA treated rats showed a significant (p < 0.05) increase in urea concentration compared to non-PTZ treated rats (Table 3). Also, PTZ/VPA, PTZ/ASTA, and PTZ/VPA/ASTA treated rats showed a significant (p < 0.05) reduction in urea concentration as compared to PTZ treated rats (Table 3).

3.3.2. Serum Tumor necrosis factor-a (TNF-α) concentration
PTZ treated rats showed a significant (p < 0.05) increase in the pro-inflammatory mediators as compared to non-PTZ treated rats (Table 3). However, PTZ/VPA/ASTA treatment resulted in a substantial reduction in TNF-α concentration compared to all other groups (Table 3). Moreover, PTZ/VPA, PTZ/ASTA, and PTZ/VPA/ASTA treated rats showed a significant (p < 0.05) reduction in TNF-α concentration compared to PTZ treated rats. Furthermore, PTZ/ASTA and PTZ/VPA/ASTA treated rats showed a significant reduction in inflammatory markers compared to PTZ/VPA treated rats (Table 3).

Y. Ata Yaseen Abdulqader, Hala Salah Abdel Kawy, H. Mohammed Alkreathy et al.

Saudi Pharmaceutical Journal 29 (2021) 418–426

3.3.3. Estimation of antioxidants, oxidative stress markers viz. GSH, MDA, PC

PTZ and PTZ/VPA treated rats showed a significant ($p < 0.05$) reduction in antioxidant levels (GSH) and a significant increase in lipid peroxidation as compared to the non-PTZ group (control) (Table 4). Moreover, all groups showed a significant ($p < 0.05$) increase in the oxidative proteins compared to the non-PTZ group. Also, VPA, ASTA, or co-treated group showed a significant ($p < 0.05$) increase in antioxidants (GSH) as compared to the PTZ treated rats. Moreover, the ASTA treated group showed a lower concentration of malondialdehyde than the PTZ group and an increase in antioxidant (GSH) compared to the PTZ/VPA group (Table 4). Furthermore, the combination group (PTZ/VPA/ASTA) showed a significant reduction in protein oxidation and MDA concentration compared to the PTZ and PTZ/VPA treated group, respectively (Table 4).

3.3.4. Reactive oxygen species concentration

As shown in Table 4, in the hippocampal tissues, PTZ and PTZ/VPA treated rats showed a significant ($p < 0.05$) increase in the reactive oxygen species levels as compared to non-PTZ treated rats (Table 4). Also, ASTA treated groups showed a significant reduction in the ROS concentration than the PTZ group.

3.3.5. Glutamate concentration estimation by HPLC

In our experiments, PTZ treatment led to a significant ($p < 0.05$) increase in the glutamate content in the hippocampal tissues in all the groups (Fig. 4). Furthermore, treatment with VPA, ASTA, or VPA/ASTA resulted in a significant ($p < 0.05$) reduction in glutamate content as compared to PTZ treated rats (Fig. 4). However, VPA/ASTA treatment had a more pronounced effect than VPA treat-ment alone (Fig. 4). However, in the cerebral cortex tissues, the PTZ group showed a significant ($p < 0.05$) increase in glutamate concentration compared to the non-PTZ group (Fig. 4).

3.4. Effects of the test drugs on histopathological changes

Histological examination of parasagittal sections of the hippocampus showed three areas of the hippocampus proper viz. CA1, CA2, and CA3 (Fig. 5). Each of these areas had three layers; polymorphic layer, pyramidal layer, and molecular layer. **Group A (negative control):-** The polymorphic layer was observed to be narrow and relatively cell free. The pyramidal layer consisted of closely packed pyramidal cells with large central vesicular nuclei and basophilic cytoplasm. The cytoplasm of the pyramidal cells appeared heavily studded with the Nissl granules. The molecular layer appeared loose, lying deep to the pyramidal layer. The astrocytes appeared as small cell bodies, with short brownish cytoplasmic processes, and more numerous in the molecular layer of areas CA1 and CA3 of the hippocampus proper (Fig. 5). **Group B (PTZ):** The cells appeared shrunken with irregular outlines and perineuronal empty spaces, deep acidophilic cytoplasm, and darkly stained nuclei. Decreased Nissl granule content was observed and the cells appeared irregular with variable sizes and ill-defined nuclei. However, few pyramidal cells had large vesicular nuclei. A higher number of GFAP positive astrocytes were observed, having larger and longer branched cytoplasmic processes (Fig. 5). **Group C (PTZ/ VPA):** The pyramidal layer cells showed central vesicular nuclei and basophilic cytoplasm. Occasional dark-stained cells were noticed in the pyramidal layer compared to the cells in group B (Epileptic model group). An apparent increase in the Nissl granules
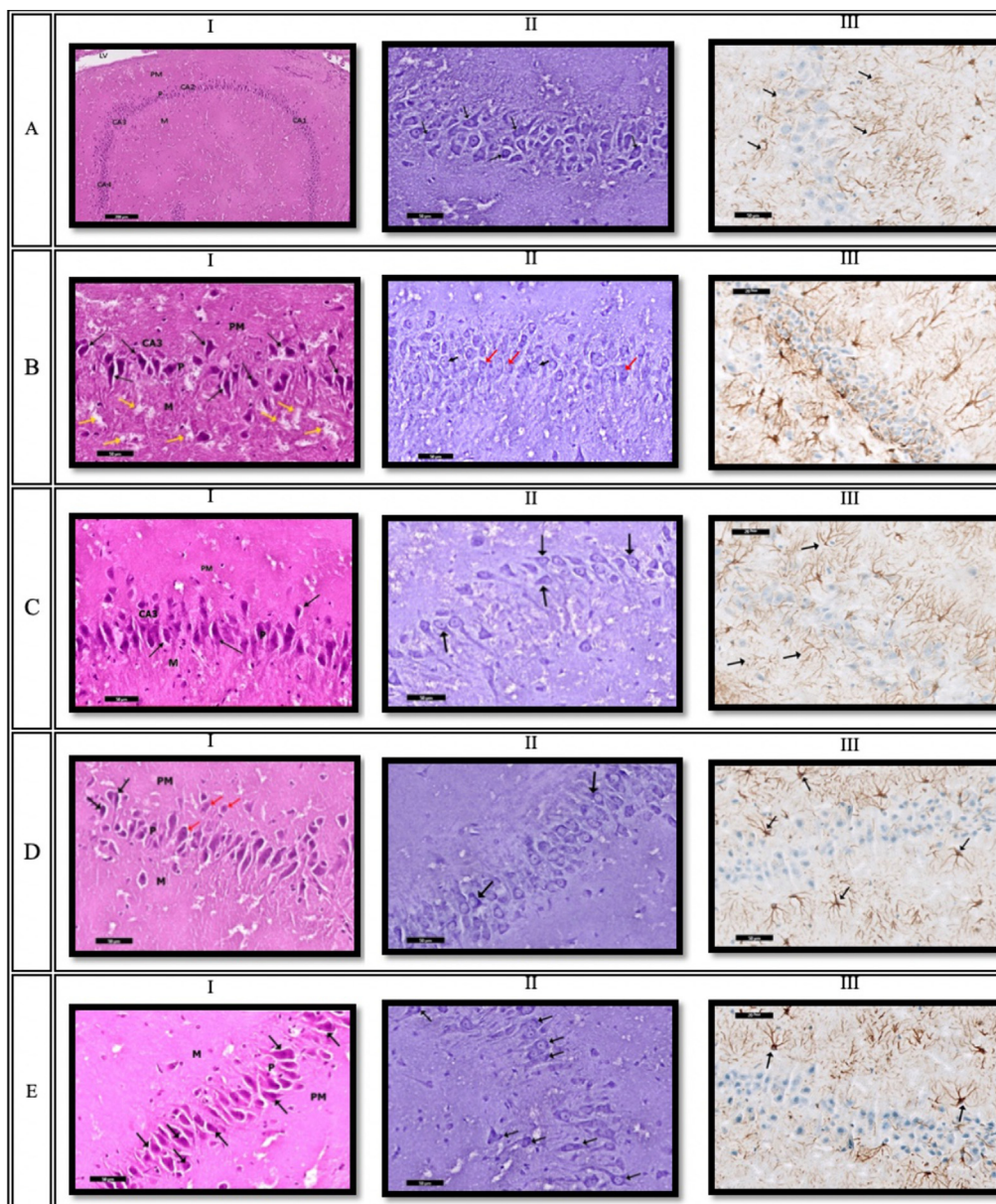
Table 4
Effect of the test drugs on antioxidants, oxidative stress markers, and ROS in hippocampal tissues measured at the end of experiment (8 weeks).

Animal groups	Hippocampus			
n = 5	GSH (ng/mg)	PC (nmol\mg)	MDA (nmol\mg)	ROS (unit\mg)
Control	118.12 ± 5.636	0.15 ± 0.029	1.16 ± 0.319	960.24 ± 28.815
PTZ	17 ± 5.409 *	1.48 ± 0.17 *	7.22 ± 0.781 *	1272.26 ± 65.075 *
VPA/PTZ	84.98 ± 8.779 *#	1.24 ± 0.112 *	6.48 ± 0.873 *	1223.58 ± 58.415 *
ASTA/PTZ	123.28 ± 5.816 #§	1.16 ± 0.094 *	4.06 ± 0.382 #	1059.24 ± 40.507 #
VPA/PTZ/ASTA	121.04 ± 3.705 # §	0.84 ± 0.214 *#	3.27 ± 0.977 #§	1056 ± 39.435 #

Data were expressed as mean ± SEM, N = number of animals. One-way ANOVA followed by Tukey multiple comparison tests. PTZ: Pentylenetetrazol, VPA: Valproic acid, ASTA: Astaxanthin. GSH: Reduced glutathione; PC: Protein carbonyl; MDA: Malondialdehyde, ROS: Reactive oxygen species.*P < 0.05 compared to control; # P < 0.05 compared to PTZ; §P < 0.05 PTZ/VPA + ASTA compared to PTZ/VPA.
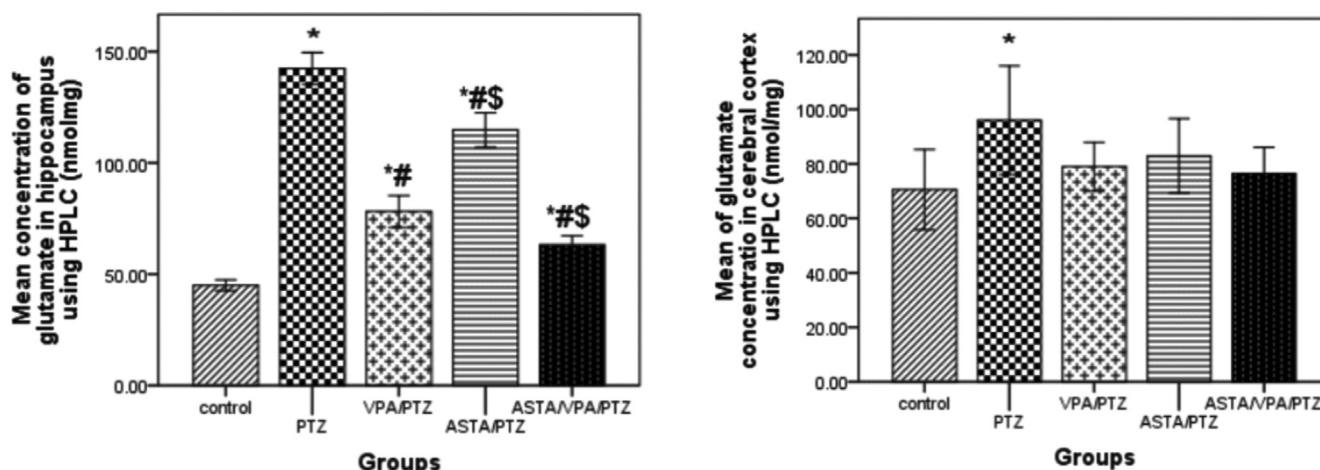
Fig. 4. Effect of the test drugs on glutamate concentration using HPLC. Data were expressed as mean ± SEM. One-way ANOVA followed by Tukey multiple comparison tests. PTZ: Pentylenetetrazol, VPA: Valproic acid, ASTA: Astaxanthin.*P < 0.05 compared to control; *#P < 0.05 compared to PTZ; *#$P < 0.05 PTZ/VPA + ASTA compared to PTZ/VPA.

Y. Ata Yaseen Abdulqader, Hala Salah Abdel Kawy, H. Mohammed Alkreathy et al.

Saudi Pharmaceutical Journal 29 (2021) 418–426

Fig. 5. Histological examination of parasagittal section of the rat hippocampus with three different staining- Hematoxylin and eosin, Nissle's, and GFAB immunohisto-chemical staining. **Hematoxylin and eosin staining:** The negative control shows normal architecture of the hippocampus **(AI)**. Notice the presence of lateral ventricle (lV). **PTZ group** shows the predominance of the degenerated deeply stained shrunken neurons with perineuronal spaces within the pyramidal layer (↑). Notice the pale vacuolated areas in the molecular layer suggesting concurrent swelling/degeneration of the pyramidal cell axons (yellow↑) **(BI)**. PTZ/ VPA group shows the presence of occasional deeply darkly stained cells (↑) **(CI)**. PTZ/ ASTA group analysis showed that most of the pyramidal cells have large rounded vesicular nuclei (red ↑). Few deeply stained cells are present with perineuronal spaces (black ↑) **(DI)**. PTZ/ VPA/ASTA group showing the pyramidal layer which is formed of the pyramidal cells (↑) with vesicular nuclei and basophilic cytoplasm **(EI)**. The outer polymorphic layer (PM), the middle pyramidal layer (P) and the inner molecular layer (M). **H&E- Scale bar 50 μm. Toluidine blue (Nissle's staining):** In the control group, the cytoplasm of the pyramidal cells appears heavily studded with Nissl granules (↑) **(AII)**. PTZ group shows an apparent decrease in the Nissl granules content (red ↑) of the pyramidal cells. The pyramidal layer with few of the pyramidal cells have large vesicular nuclei (black ↑) are seen **(BII)**. PTZ/ VPA **group** shows an apparent increase in the Nissl granules content (↑) **(CII)**. PTZ/ ASTA group shows an apparent moderate increase in the Nissl granules content (↑) **(DII)**. PTZ/ VPA/ ASTA group shows an apparent increase in the Nissl granules content (↑) **(EII)**. **Toluidine blue- Scale bar 50 μm. GFAB immunohistochemical staining:** Control group shows positive reaction for GFAP immuno-staining in the cytoplasm of astrocytes (↑) **(AIII)**. PTZ shows an apparent increase of the positive brownish reaction for GFAP immuno-staining in the cytoplasm of astrocytes **(BIII)**. PTZ/VPA shows an apparent decrease of the positive brownish reaction for GFAP immuno-staining in the cytoplasm of the astrocytes. Notice that astrocytes present shorter processes (↑) **(CIII)**. PTZ/ ASTA showing the apparent moderate decrease of the positive brownish reaction for GFAP immuno-staining in the cytoplasm of the astrocytes **(DIII)**. PTZ/VPA/ASTA group shows an apparent decrease of the positive brownish reaction for GFAP immuno-staining in the cytoplasm of the astrocytes **(EIII)**. **Avidin–biotin technique- Scale 50 μm.**

content was observed with decreased intensity of GFAB, and the astrocytes in the CA3 region presented shorter cytoplasmic processes compared to that of group B (Fig. 5). **Group D (PTZ/ASTA):** The pyramidal layer showed moderate improvement in histological structure. The number of pyramidal cells increased, and they exhibited large rounded vesicular nuclei. The cells also showed

an apparent moderate increase in the Nissl granules content, while GFAP demonstrated a moderate decrease in the number of astrocytes in area CA3. The astrocytes were small in size with few short branched processes (Fig. 5). **Group E (PTZ/VPA/ASTA):** The pyramidal cells showed improvement in their histological structure along with an increase in cell number as compared to group C **(PTZ/VPA)**

and also exhibited large rounded vesicular nuclei (Fig. 5). Few degenerated neurons with deeply stained cytoplasm and perineuronal spaces were observed. Also, an apparent increase in the Nissl granules content was observed, while GFAP demonstrated a decrease in the number of astrocytes. The astrocytes were small in size with few short branched processes compared to that of group C **(PTZ/VPA)** (Fig. 5).

4. Discussion

In the present study, PTZ treatment induced continuous seizure activity in rats with a significant increase in average Racine score. The PTZ/VPA group showed antiepileptic activity with reduced glutamate concentration, confirming the neuroprotective effect of VPA against PTZ kindling seizures. Similarly, Sefil et al. (2015) reported that VPA completely prevented the occurrence of generalized seizures (Sefil et al., 2015). However, the efficacy of AED decreases over time, as evident from a gradual increase in Racine scores. It could be because of tolerance and/or resistance induced by disease-related mechanisms, such as drug movement inhibition across the blood–brain barrier (BBB) (Cardenas-Rodriguez et al., 2013). This pharmaco-resistance minimized the anticonvulsant effect of VPA and also enhanced ROS production. Martinc et al. (2012) also noted that prolonged use of certain AEDs causes oxidative damage to neurons and ultimately increases pharmaco-resistance (Martinc et al., 2012). Additionally, AED treatment itself may exacerbate epilepsy by increasing ROS production or reducing endogenous antioxidants' synthesis. First-generation of antiepileptic drugs such as valproic acid increases ROS production by triggering oxygen dependent tissue injury.

In our study, astaxanthin (ASTA) exhibited an anticonvulsant effect against PTZ-induced kindling and improved motor coordination. ASTA can easily cross the BBB to reach effective concentration levels (Ambati et al., 2014; Deng et al., 2019). Supporting our results, (Deng et al. (2019) study revealed that ASTA inhibits seizure severity and restores behavioral activity in animals (Deng et al., 2019). ASTA treated group showed lower glutamate concentration reduction in the hippocampus as compared to VPA groups, possibly because ASTA treatment does not affect the glutamate receptors. Nonetheless, ASTA treatment decreases ROS production, minimizes glutamate induction, and suppresses NO synthase activity. Significantly, seizures lead to neuronal degeneration due to resultant excitotoxicity and increased glutamatergic transmission (Mohammed et al., 2014). Additionally, a recent study clearly showed that oral ASTA treatment prevented the loss of cortical neurons and associated behavioral impairments in mice after traumatic brain injury (Ji et al., 2017).

Interestingly, PTZ/VPA/ASTA group showed better anticonvulsant effect than VPA and ASTA groups alone, leading to prolonged latency to onset of GTCS. Similarly, (Chang et al. (2018) noted that ASTA pretreatment increased the latency period of seizure development and also reduced the seizure score (Chang et al., 2018). Furthermore, VPA/ASTA combination treatment significantly reduced the glutamate concentration as compared to the VPA group. These results revealed that ASTA has a synergistic effect with VPA, where VPA acts as a glutamate antagonist, and ASTA reduces ROS and nitric oxide generation, thereby potentiating the effect of VPA.

VPA treatment increased oxidative stress and ROS, and reduced GSH levels. It could be because of large calcium influx leading to biochemical cascades, which stimulates ROS production leading to acute neuronal death (Fujikawa et al., 2000). (Reeta et al. (2011) reported similar results where valproic acid increased MDA level and decreased GSH level in epileptic rats (Reeta et al., 2011). On long-term use, VPA has shown to increase oxidative stress and lipid peroxidation, possibly through its metabolism to release reactive epoxide intermediates (Martinez-Ballesteros et al., 2004). In contrast, histopathological changes improved in PTZ/VPA treated group, indicative of its neuroprotective effect. Sedky et al. (2017) also reported that VPA treatment resulted in amelioration during the histopathological investigations (Sedky et al., 2017).

Interestingly, in the present study, ASTA downregulated MDA and PC levels and upregulated GSH levels in the hippocampus tissue, corroborating with a recent study (Deng et al., 2019). An important finding of our study is that PTZ/ASTA and PTZ/VPA/ASTA treated groups showed a significant reduction in ROS concentration. These findings explain the earlier reported anticonvulsant and neuroprotective effect of ASTA (Fujikawa et al., 2000). ASTA treatment attenuates the neuronal damage by decreasing ROS and MDA levels, increasing GSH levels, and inhibiting the apoptotic pathways (Lu et al., 2015). Moreover, ASTA groups showed an improvement in the histopathological structure, which was also reported recently (Deng et al., 2019). ASTA can also effectively cross the BBB, conferring neuroprotection against the neural and oxidative damage caused by MDA and ROS (Manabe et al., 2018). In the same study, ASTA treatment also prevented neuronal loss by inhibiting mitochondrial-mediated apoptosis pathways.

In CNS, TNF-α is mainly produced by activated microglia and astrocytes in response to various stimuli, including infection and injury (Liu et al., 2014). In our study too, PTZ treatment showed a significant increase in TNF-α levels. An earlier study demonstrated that seizures induced by PTZ might also result in changes in nitric oxide metabolism (Naziroglu et al., 2009). These pro-inflammatory elements exacerbate the proliferation of neuroglial cells, harm the BBB, and induce neuronal excitability and seizure intensity, which adds to the neuronal loss.

VPA treatment reduced TNF-α levels, showing some anti-inflammatory effect, but lesser than ASTA. Elsherbiny et al. (2019) also reported that VPA suppresses histone deacetylase 1 and inflammatory mediators such as TNF-α and IL-1b (Elsherbiny et al., 2019). They also revealed that VPA induced pain killing action is through the suppression of histone deacetylase 1 and inflammatory mediator such as TNF-α and IL-1b.

Similarly, the ASTA group also showed a substantial reduction in the TNF-α levels. These results corroborate with an earlier study where ASTA treatment reduced inflammatory factors like IL-1b, and TNF-α (Kim et al., 2017). Moreover, the co-administration of VPA and ASTA also reduced TNF-α, further highlighting the anti-inflammatory effect of ASTA. PTZ/VPA group showed a significant increase in urea, which was observed in a similar study (Abdel-Dayem et al., 2014). The proposed mechanism for VPA-induced accumulation of ammonia is by reducing free carnitine and coenzyme A in the hepatic cells' mitochondria (Beheshti et al., 2016). However, VPA increases renal uptake of glutamate, as is evident from the lower glutamate concentration observed in the cerebral cortex tissue of the PTZ/VPA group, which further supports the neuroprotective role of VPA.

A limitation of the current study is the small sample size and absence of the control group that received VPA alone to measure VPA-induced hepatotoxicity. Nonetheless, it is recommended to study the effect of ASTA on the patients with VPA pharmaco-resistance genotypes, toxicity and interaction studies of long-term therapy use of ASTA and VPA together.

5. Conclusion

Valproic acid is a commonly used antiepileptic drug with a neuroprotective effect. However, prolonged use of valproic acid leads to an increase in the ROS levels, leading to recurrent seizures.

Y. Ata Yaseen Abdulqader, Hala Salah Abdel Kawy, H. Mohammed Alkreathy et al.

Saudi Pharmaceutical Journal 29 (2021) 418–426

Astaxanthin is a powerful antioxidant that reduces the impact of oxidative stress without any harmful side effects. It also decreases the ROS generation and suppresses pro-inflammatory mediators. Overall, valproic acid and astaxanthin's co-administration has a synergistic effect, potentiating the effect of valproic acid as an effective anticonvulsant.

Declaration of Competing Interest

The authors declare that they have no known competing financial interests or personal relationships that could have appeared to influence the work reported in this paper.

Acknowledgment

References

Abdel-Dayem, M.A., Elmarakby, A.A., Abdel-Aziz, A.A., Pye, C., Said, S.A., El-Mowafy, A.M., 2014. Valproate-induced liver injury: modulation by the omega-3 fatty acid DHA proposes a novel anticonvulsant regimen. Drugs. R. D. 14, 85–94. https://doi.org/10.1007/s40268-014-0042-z.

Al-Qahtani, M.A., Amin, H.S., Al-Qahtani, A.A., Alshahrani, A.M., Alghamdi, H.A., Althwayee, M.S., Alzahrani, A.A., 2018. Self-medication with Antibiotics in a primary care setting in King Khalid University Hospital, Riyadh, Saudi Arabia. J. Family. Community. Med. 25, 95–101. https://doi.org/10.4103/jfcm.JFCM_124_17.

Althobaiti, Y.S., Almalki, A.H., Das, S.C., Alshehri, F.S., Sari, Y., 2016. Effects of repeated high-dose methamphetamine and ceftriaxone post-treatments on tissue content of dopamine and serotonin as well as glutamate and glutamine. Neurosci. Lett. 634, 25–31. https://doi.org/10.1016/j.neulet.2016.09.058.

Ambati, R.R., Phang, S.M., Ravi, S., Aswathanarayana, R.G., 2014. Astaxanthin: sources, extraction, stability, biological activities and its commercial applications–a review. Mar. Drugs. 12, 128–152. https://doi.org/10.3390/md12010128.

Atack, J.R., Cook, S.M., Hutson, P.H., File, S.E., 2000. Kindling induced by pentylenetetrazole in rats is not directly associated with changes in the expression of NMDA or benzodiazepine receptors. Pharmacol. Biochem. Behav. 65, 743–750. https://doi.org/10.1016/s0091-3057(99)00267-1.

Beheshti, F., Khazaei, M., Hosseini, M., 2016. Neuropharmacological effects of Nigella sativa. Avicenna. J. Phytomed. 6, 104–116.

Cardenas-Rodriguez, N., Huerta-Gertrudis, B., Rivera-Espinosa, L., Montesinos-Correa, H., Bandala, C., Carmona-Aparicio, L., Coballase-Urrutia, E., 2013. Role of oxidative stress in refractory epilepsy: evidence in patients and experimental models. Int. J. Mol. Sci. 14, 1455–1476. https://doi.org/10.3390/ijms14011455.

Chang, Y., Lu, C.W., Chen, Y.J., Lin, T.Y., Huang, S.K., Wang, S.J., 2018. Astaxanthin protects against kainic acid-induced seizures and pathological consequences. Neurochem. 116, 85–94. https://doi.org/10.1016/j.neuint.2018.02.008.

Deng, X., Wang, M., Hu, S., Feng, Y., Shao, Y., Xie, Y., Wu, M., Chen, Y., Shi, X., 2019. The neuroprotective effect of astaxanthin on pilocarpine-induced status epilepticus in rats. Front. Cell. Neurosci. 13, 123. https://doi.org/10.3389/fncel.2019.00123.

El-Mowafy, A.M., Katary, M.M., Pye, C., Ibrahim, A.S., Elmarakby, A.A., 2016. Novel molecular triggers underlie valproate-induced liver injury and its alleviation by the omega-3 fatty acid DHA: role of inflammation and apoptosis. Heliyon. 2,. https://doi.org/10.1016/j.heliyon.2016.e00130 e00130.

Elsherbiny, N.M., Ahmed, E., Kader, G.A., Abdel-Mottaleb, Y., ElSayed, M.H., Youssef, A.M., Zaitone, S.A., 2019. Inhibitory effect of valproate sodium on pain behavior in diabetic mice involves suppression of spinal histone deacetylase 1 and inflammatory mediators. Int. Immunopharmacol. 70, 16–27. https://doi.org/10.1016/j.intimp.2019.01.050.

Fujikawa, D.G., Itabashi, H.H., Wu, A., Shinmei, S.S., 2000. Status epilepticus-induced neuronal loss in humans without systemic complications or epilepsy. Epilepsia. 41, 981–991. https://doi.org/10.1111/j.1528-1157.2000.tb00283.x.

Grewal, G.K., Kukal, S., Kanojia, N., Saso, L., Kukreti, S., Kukreti, R., 2017. Effect of oxidative stress on ABC transporters: contribution to epilepsy

pharmacoresistance. Molecules 22. https://doi.org/10.3390/molecules22030365.

Huang, L.T., Yang, S.N., Liou, C.W., Hung, P.L., Lai, M.C., Wang, C.L., Wang, T.J., 2002. Pentylenetetrazol-induced recurrent seizures in rat pups: time course on spatial learning and long-term effects. Epilepsia. 43, 567–573. https://doi.org/10.1046/j.1528-1157.2002.29101.x.

Jentink, J., Loane, M. A., Dolk, H., Barisic, I., Garne, E., Morris, J.K., de Jong-van den Berg, L.T., Group, E.A.S.W., 2010. Valproic acid monotherapy in pregnancy and major congenital malformations. N. Engl. J. Med. 362, 2185–2193. 10.1056/NEJMoa0907328

Ji, X., Peng, D., Zhang, Y., Zhang, J., Wang, Y., Gao, Y., Lu, N., Tang, P., 2017. Astaxanthin improves cognitive performance in mice following mild traumatic brain injury. Brain. Res. 1659, 88–95. https://doi.org/10.1016/j.brainres.2016.12.031.

Kim, B., Farruggia, C., Ku, C.S., Pham, T.X., Yang, Y., Bae, M., Wegner, C.J., Farrell, N.J., Harness, E., Park, Y.K., et al., 2017. Astaxanthin inhibits inflammation and fibrosis in the liver and adipose tissue of mouse models of diet-induced obesity and nonalcoholic steatohepatitis. J. Nutr. Biochem. 43, 27–35. https://doi.org/10.1016/j.jnutbio.2016.01.006.

Liu, S., Wang, X., Li, Y., Xu, L., Yu, X., Ge, L., Li, J., Zhu, Y., He, S., 2014. Necroptosis mediates TNF-induced toxicity of hippocampal neurons. Biomed. Res. Int. 2014,. https://doi.org/10.1155/2014/290182 290182.

Lowry, O.H., Rosebrough, N.J., Farr, A.L., Randall, R.J., 1951. Protein measurement with the Folin phenol reagent. J. Biol. Chem. 193, 265–275.

Lu, Y., Xie, T., He, X.X., Mao, Z.F., Jia, L.J., Wang, W.P., Zhen, J.L., Liu, L.M., 2015. Astaxanthin rescues neuron loss and attenuates oxidative stress induced by amygdala kindling in adult rat hippocampus. Neurosci. Lett. 597, 49–53. https://doi.org/10.1016/j.neulet.2015.04.018.

Manabe, Y., Komatsu, T., Seki, S., Sugawara, T., 2018. Dietary astaxanthin can accumulate in the brain of rats. Biosci. Biotechnol. Biochem. 82, 1433–1436. https://doi.org/10.1080/09168451.2018.1459467.

Martinc, B., Grabnar, I., Vovk, T., 2012. The role of reactive species in epileptogenesis and influence of antiepileptic drug therapy on oxidative stress. Curr. Neuropharmacol. 10, 328–343. https://doi.org/10.2174/157015912804143504.

Martinez-Ballesteros, C., Pita-Calandre, E., Sanchez-Gonzalez, Y., Rodriguez-Lopez, C.M., Agil, A., 2004. Lipid peroxidation in adult epileptic patients treated with valproic acid. Rev. Neurol. 38, 101–106.

Mendez-Armenta, M., Nava-Ruiz, C., Juarez-Rebollar, D., Rodriguez-Martinez, E., Gomez, P.Y., 2014. Oxidative stress associated with neuronal apoptosis in experimental models of epilepsy. Oxid. Med. Cell. Longev. 2014,. https://doi.org/10.1155/2014/293689 293689.

Mohammed, A.S., Ewais, M.M., Tawfik, M.K., Essawy, S.S., 2014. Effects of intravenous human umbilical cord blood mesenchymal stem cell therapy versus gabapentin in pentylenetetrazole-induced chronic epilepsy in rats. Pharmacology 94, 41–50. https://doi.org/10.1159/000365219.

Naziroglu, M., Kutluhan, S., Uguz, A.C., Celik, O., Bal, R., Butterworth, P.J., 2009. Topiramate and vitamin e modulate the electroencephalographic records, brain microsomal and blood antioxidant redox system in pentylenetetrazol-induced seizure of rats. J. Membr. Biol. 229, 131–140. https://doi.org/10.1007/s00232-009-9177-1.

Nita, M., Grzybowski, A., 2016. The role of the reactive oxygen species and oxidative stress in the pathomechanism of the age-related ocular diseases and other pathologies of the anterior and posterior eye segments in adults. Oxid. Med. Cell. Longev. 2016, 3164734. https://doi.org/10.1155/2016/3164734.

World Health Organization, 2019. Epilepsy: a public health imperative Retrieved from https://www.who.int/mental_health/neurology/epilepsy/report_2019/en/ . .

Racine, R.J., 1972. Modification of seizure activity by electrical stimulation. II. Motor seizure. Electroencephalogr. Clin. Neurophysiol. 32, 281–294. https://doi.org/10.1016/0013-4694(72)90177-0.

Reeta, K.H., Mehla, J., Pahuja, M., Gupta, Y.K., 2011. Pharmacokinetic and pharmacodynamic interactions of valproate, phenytoin, phenobarbitone and carbamazepine with curcumin in experimental models of epilepsy in rats. Pharmacol. Biochem. Behav. 99, 399–407. https://doi.org/10.1016/j.pbb.2011.05.011.

Rowley, S., Liang, L.P., Fulton, R., Shimizu, T., Day, B., Patel, M., 2015. Mitochondrial respiration deficits driven by reactive oxygen species in experimental temporal lobe epilepsy. Neurobiol. Dis. 75, 151–158. https://doi.org/10.1016/j.nbd.2014.12.025.

Sedky, A.A., El Serafy, O.M.H., Hassan, O.A., Abdel-Kawy, H.S., Hasanin, A.H., Raafat, M.H., 2017. Trimetazidine potentiates the antiepileptic activity and ameliorates the metabolic changes associated with pentylenetetrazole kindling in rats treated with valproic acid. Can. J. Physiol. Pharmacol. 95, 686–696. https://doi.org/10.1139/cjpp-2016-0263.

Sefil, F., Arik, A.E., Acar, M.D., Bostanci, M.O., Bagirici, F., Kozan, R., 2015. Interaction between carbenoxolone and valproic acid on pentylenetetrazole kindling model of epilepsy. Int. J. Clin. Exp. Med. 8, 10508–10514.

Shin, E.J., Jeong, J.H., Chung, Y.H., Kim, W.K., Ko, K.H., Bach, J.H., Hong, J.S., Yoneda, Y., Kim, H.C., 2011. Role of oxidative stress in epileptic seizures. Neurochem. Int. 59, 122–137. https://doi.org/10.1016/j.neuint.2011.03.025.